

Detecting the QCD phase transition in the next Galactic supernova neutrino burst

Basudeb Dasgupta,¹ Tobias Fischer,² Shunsaku Horiuchi,^{3,4} Matthias Liebendörfer,² Alessandro Mirizzi,⁵ Irina Sagert,^{6,7} and Jürgen Schaffner-Bielich⁷

¹*Max-Planck-Institut für Physik (Werner-Heisenberg-Institut), Föhringer Ring 6, 80805 München, Germany*

²*Department of Physics, University of Basel, Klingelbergstr. 82, CH-4056 Basel, Switzerland*

³*Institute for the Physics and Mathematics of the Universe,*

University of Tokyo, 5-1-5, Kashiwanoha, Kashiwa, Chiba 277-8582, Japan

⁴*Center for Cosmology and Astro-Particle Physics, Ohio State University, Columbus, Ohio 43210*

⁵*II Institut für Theoretische Physik, Universität Hamburg,*

Luruper Chaussee 149, 22761 Hamburg, Germany

⁶*Institut für Theoretische Physik, Goethe Universität,*

Max-von-Laue-Str. 1, 60438 Frankfurt am Main, Germany

⁷*Institut für Theoretische Physik, Ruprecht-Karls-Universität, Philosophenweg 16, 69120 Heidelberg, Germany*

(Dated: February 7, 2020)

Observations of core-collapse supernovae can be used to probe the quark-hadron phase transition at high baryon densities. Recent simulations of stellar core-collapse that include descriptions of quark matter predict a sharp burst of $\bar{\nu}_e$ several hundred milliseconds after the prompt ν_e neutronization burst. We study the observational signatures of the $\bar{\nu}_e$ burst at the current neutrino detectors IceCube and Super-Kamiokande, and find that a QCD phase transition in a Galactic core-collapse can clearly be detected, regardless of the neutrino oscillation scenario. The detection would constitute direct evidence of quark matter in the neutron star and would have significant implications for our understanding of supernovae and the state of matter at extreme conditions.

PACS numbers: 14.60.Pq, 26.50.+x, 95.85.Ry, 97.60.Bw

Introduction.— The majority of stars more massive than $8 M_\odot$ end their lives as core-collapse supernovae (SNe) with explosive kinetic energies $\sim 10^{51}$ erg. The explosion mechanism is related to the revival of the stalled bounce shock – the shock that forms when the collapsing iron core reaches nuclear densities and bounces back, and continuously loses energy due to neutrinos and the dissociation of heavy nuclei. Direct observables are limited, since the matter envelope is opaque for photons and nucleosynthesis analyses of the ejecta are model dependent. Neutrinos from SNe have therefore been highly sought after for providing valuable information on the SN mechanism. Indeed, the diffuse neutrino background from all past SNe is on the verge of detection [1, 2, 3], and current neutrino detectors are expecting high statistics from the next Galactic SN. This would enable the explosion mechanism to be tested [4, 5, 6, 7], as well as neutrino mixing parameters to be constrained [8]. Moreover, the neutrinos send a record of the physical conditions and dynamics of the collapse to the distant observer, potentially revealing new physics deep in the stellar core.

The quark-hadron phase transition has long been investigated in the context of SNe [9] and protonneutron stars [10]. The first attempt was based on general relativistic hydrodynamics using a parametrized equation of state (EoS) [9], discussing a possible relation to the neutrino spectrum from SN1987A [11]. Applying a more sophisticated EoS and deleptonization scheme for the emission of electron neutrinos during the collapse phase of massive progenitor stars, the formation of a strong second shock wave was found as a direct consequence of

the phase transition [12]. However, both studies could not predict the post-bounce neutrino signal due to the lack of neutrino transport. The QCD phase transition has also been investigated in the context of very massive ($\sim 100 M_\odot$) progenitor stars that collapse to black holes. It has been shown that the time until black hole formation is shortened due to the softening of the EoS during the quark-hadron phase transition [13]. Recently, applying general relativistic radiation hydrodynamics based on three-flavor Boltzmann neutrino transport in spherically-symmetric simulations of low- and intermediate-mass progenitor stars, combined with the MIT bag model for the description of strange quark matter, the formation of a strong second shock wave was confirmed [14]. The second shock accelerates at the surface of the protonneutron star and merges with the bounce shock, triggering an explosion where otherwise no explosion could be obtained. As the second shock crosses the neutrinosphere, a second burst of neutrinos is released. Due to the non-degeneracy of the shock-heated material, this second burst is dominated by $\bar{\nu}_e$.

Current neutrino detectors like IceCube and Super-Kamiokande are mostly sensitive to SN $\bar{\nu}_e$ through inverse beta decay reactions ($\bar{\nu}_e p \rightarrow n e^+$) in the detector medium, while ν_e are detected by the subleading elastic scattering channel. Encouragingly, the second burst, associated with the QCD phase transition, shows up most prominently in $\bar{\nu}_e$, and its detection appears feasible already. This contrasts with the deleptonization burst which has been widely explored and proposed as a crucial tool to determine the flavor oscillation effects on the SN

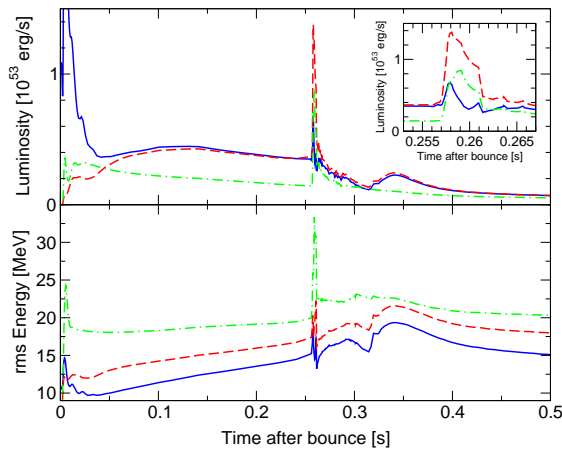


FIG. 1: Neutrino luminosities and rms neutrino energies as functions of time after bounce, sampled at 500 km radius in the comoving frame, for a $10 M_{\odot}$ progenitor star: ν_e in solid (blue), $\bar{\nu}_e$ in dashed (red), and $\nu_{\mu/\tau}$ in dot-dashed (green). In contrast to the deleptonization burst just after bounce ($t \sim 5$ ms) the second burst at $t \sim 257 - 261$ ms is associated with the QCD phase transition. The inset shows the second burst blown up.

neutrino signal [15, 16]; since the neutronization burst consists of ν_e , its detection requires larger neutrino experiments. If the QCD $\bar{\nu}_e$ burst is observed, it would constitute a smoking-gun signature for the presence of a phase transition in the SN core, with important implications for SN input physics. We consider this intriguing possibility and investigate the capabilities of the largest existing neutrino detectors to measure the QCD phase transition $\bar{\nu}_e$ burst from a galactic SN (assumed at a distance of 10 kpc unless otherwise stated).

Numerical model.— We employ the neutrino emission obtained from core-collapse simulations of massive stars [14], shown in Fig. 1. One recognizes the ordinary deleptonization burst in the ν_e signal at $t \simeq 5$ ms after bounce. The inclusion of the QCD phase transition gives rise to a second burst, comprising of $\bar{\nu}_e$, at about the time when the quark matter core is created ($t \simeq 260$ ms for the simulation shown in the Fig. 1). The luminosity increases by factors of 2 – 4 depending on the neutrino flavor. The duration of the second burst is ~ 4 ms and the time-integrated energetics is approximately 5×10^{50} erg in $\bar{\nu}_e$, $\sim 1\%$ of the total energetics. The burst is also accompanied by a sharp rise in the neutrino average energies. The oscillatory behavior of the neutrino lightcurve shortly after the second burst is due to the appearance of an oscillating accretion shock caused by neutrino cooling, since the electron flavor neutrino luminosities are driven by mass accretion at the neutrinospheres. However, on a timescale of about 100 ms after the second burst, the oscillating accretion shock settles down to a quasi-stationary state where the electron flavor neutrino luminosities follow accordingly.

The delay of the second burst after the deleptonization burst contains correlated information about the hadron EoS (compressibility of nuclear matter), the critical conditions for the quark-hadron phase transition, and the progenitor model. A second set of simulations using a larger bag constant results in a higher critical density, which delays the post-bounce time for the second burst by ~ 100 ms (see Table I of Ref. [14]). Otherwise, the burst duration (~ 4 ms) and energetics ($\sim 10^{50}$ erg in $\bar{\nu}_e$) are similar to those shown in Fig. 1.

Neutrino flavor conversions.— In order to determine the SN $\bar{\nu}_e$ signal observed at Earth, one has to take into account flavor conversions occurring during propagation in the stellar matter. In general, neutrino oscillation effects vary during the post-bounce evolution. In particular, collective flavor conversions in the SN [17] are forbidden during the protonization burst. From Fig. 1, one realizes that during this phase the $\bar{\nu}_e$ flux is strongly enhanced with respect to the non-electronic species ν_x and $\bar{\nu}_x$ (where $x = \mu, \tau$) while the ν_e flux is strongly suppressed. In this condition, the conservation of the lepton number prevents the collective $\nu_e \bar{\nu}_e \rightarrow \nu_x \bar{\nu}_x$ pair conversions [18]. Therefore, only Mikheyev-Smirnov-Wolfenstein (MSW) flavor conversions occur while neutrinos propagate in the stellar envelope [19]. In inverted mass hierarchy ($m_3 < m_1 < m_2$, where m_i is the neutrino mass state), MSW matter effects in the SN envelope are characterized in terms of the level-crossing probability P_H of antineutrinos, which is in general a function of the neutrino energy and of the 1–3 leptonic mixing angle θ_{13} [19]. In the following, we consider two extreme limits, namely $P_H \simeq 0$ when $\sin^2 \theta_{13} \gtrsim 10^{-3}$ (large) and $P_H \simeq 1$ when $\sin^2 \theta_{13} \lesssim 10^{-5}$ (small). Neglecting for simplicity Earth matter crossing effects, the electron antineutrino flux $F_{\bar{\nu}_e}$ at the Earth surface for inverted hierarchy with small θ_{13} , is given in terms of the primary fluxes F_{ν}^0 by [19]

$$F_{\bar{\nu}_e} \simeq \cos^2 \theta_{12} F_{\bar{\nu}_e}^0 + \sin^2 \theta_{12} F_{\bar{\nu}_x}^0, \quad (1)$$

where $\cos^2 \theta_{12} \simeq 2/3$, θ_{12} being the “solar” mixing angle [20]. For inverted hierarchy with large θ_{13} one has

$$F_{\bar{\nu}_e} \simeq F_{\bar{\nu}_x}^0. \quad (2)$$

For normal mass hierarchy ($m_1 < m_2 < m_3$) the expression in Eq. (1) is applicable.

The signal is thus expected to be larger for inverted mass hierarchy and small θ_{13} (or normal mass hierarchy) than that for inverted hierarchy with large θ_{13} , because $F_{\bar{\nu}_e}^0 > F_{\bar{\nu}_x}^0$.

Outside the $\bar{\nu}_e$ burst, one has $F_{\nu_e}^0 > F_{\bar{\nu}_e}^0 > F_{\nu_x}^0$. This flux ordering allows for both collective and matter flavor transitions in inverted mass hierarchy. Now $F_{\bar{\nu}_e}$ is given by Eq. (1) for large θ_{13} , and Eq. (2) for small θ_{13} , i.e., effectively the case of large and small θ_{13} are exchanged relative to the case with no collective effects. Collective

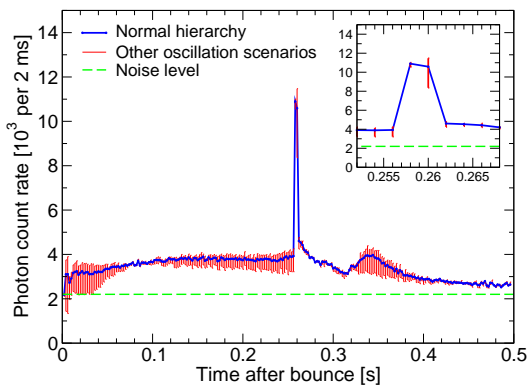


FIG. 2: Photon count rates at IceCube for the neutrino emission shown in Fig. 1. The solid line (blue) represents the signal for normal hierarchy, and the vertical band (red) shows the range in the predicted signal due to different neutrino oscillation scenarios. The horizontal dashed line (green) is the constant background noise. Time bins of 2 ms have been used. The inset shows the second burst blown up, in the same axis units.

oscillations do not occur significantly in normal hierarchy (unless ν_x or $\bar{\nu}_x$ have relatively large fluxes, which is not the case here) and we find as the final flux the same result of Eq. (1).

Detection of the QCD neutrino burst.— We analyze the detection of the QCD phase transition induced $\bar{\nu}_e$ burst in two neutrino detectors, the km³ ice Čerenkov detector IceCube and the 32 kton water Čerenkov detector Super-Kamiokande. The detectors have distinct advantages – IceCube is greater in volume, while Super-Kamiokande allows spectral energy reconstruction.

We utilize the full spectrum produced by numerical simulations. To estimate the event rate produced by inverse- β decay in the ice, we follow the recent calculation of Halzen and Raffelt [7]. The complete detector will have 4800 optical modules and the data are read out in 1.6384 ms bins, implying a total event rate of $R_{\bar{\nu}_e} = 1860 \text{ bin}^{-1} L_{53} d_{10}^{-2} \langle E_{15}^3 \rangle / \langle E_{15} \rangle^3$, where L_{53} is the $\bar{\nu}_e$ luminosity in units of $10^{53} \text{ erg s}^{-1}$, d is the distance to the SN in units of 10 kpc, and E_{15} is the $\bar{\nu}_e$ energy in units of 15 MeV. The last factor in the expression is about 1.8 in our case. The signal rate has to be compared with the stochastic background rate $R_0 = 2.20 \times 10^3 \text{ bin}^{-1}$, with an rms fluctuation of 47 bin^{-1} . In Fig. 2 we show the event rate due to the $\bar{\nu}_e$ burst in IceCube for normal mass hierarchy [Eq. (1)]. In the narrow time window (~ 4 ms) where the burst would show up, one would collect $\sim 2 \times 10^4$ events, as opposed to 8000 for the simulation without the QCD phase transition.

The vertical band (red) corresponds to the range of allowed signals for other possible oscillation scenarios. If we take the most pessimistic possibility that the oscillation effects are somehow arranged to produce the maximum possible signal outside the burst region and the minimum

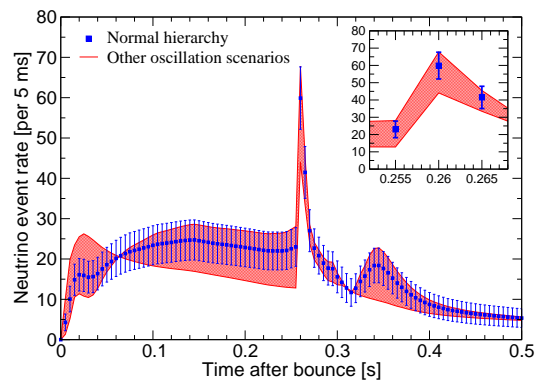


FIG. 3: Reconstructed neutrino event rates (note the subtle difference from Fig. 2) at Super-Kamiokande, for the neutrino emission shown in Fig. 1. The square points (blue) represent the event rates for the normal hierarchy, binned at 5 ms. The error bars show statistical errors. The shaded band (red) represents the range of predicted neutrino event rates due to different neutrino oscillation scenarios. The inset shows the second burst blown up, in the same axis units.

possible inside it, we still get $\sim 10^4$ additional events in the burst bins over a steady background of $\sim 10^4$ SN events producing an excess with a significance of $\sim 100\sigma$. The significance goes down at most quadratically with the SN distance, but note that even a SN at 50 kpc (the LMC) would provide a hugely significant signal. Thus even in the most pessimistic scenario, the signature of the $\bar{\nu}_e$ burst, associated with the QCD phase transition in the SN core, would be spectacular in IceCube.

Secondly, since the temporal position of the $\bar{\nu}_e$ burst depends on the EoS and critical conditions for the phase transition, reconstructing the post-bounce time of the $\bar{\nu}_e$ burst is crucial. IceCube can reconstruct the bounce time to within ± 3.5 ms at 95% CL for a SN at 10 kpc [7]. The data at IceCube are read out at 1.6384 ms bins, hence the post-bounce time of the QCD burst may be measured to within about ± 4 ms, which is sufficiently accurate to decipher between different predictions of the post-bounce times of the $\bar{\nu}_e$ burst (see, e.g., Table I of Ref. [14]).

Next we investigate the detection at Super-Kamiokande. The simplest procedure to perform is to similarly time-bin the events. We use bins of 5 ms, which is comparable to the duration of the second burst. Fig. 3 shows the reconstructed neutrino event rates expected in Super-Kamiokande for the normal mass hierarchy in square points (blue) with statistical error bars. The range of allowed rates for other possible oscillation scenarios is shown by the shaded band (red). The QCD burst would produce ~ 60 excess events in the two relevant bins, over the ~ 50 events coming from the standard SN signal, for the normal mass hierarchy. The statistics are encouraging enough that the QCD-burst would be identifiable even at a SN distance of 20 kpc, which would contain $\sim 90\%$ of the Galactic SNe [22].

However, the smaller the signal to noise ratio, the larger the risk that fluctuations in the accretion flow, which also produce variations in the electron flavor neutrino luminosities (see, e.g., [23]) can obscure a clear signal of the phase transition.

Super-Kamiokande's energy resolution can reveal a second distinguishing feature of the QCD phase transition burst – the increase of the average neutrino energies. In particular, the largest energy increase is seen in the $\bar{\nu}_x$, which rapidly increases from 20 MeV to 35 MeV (see Fig. 1). For the inverted mass hierarchy with large θ_{13} , this energy increase would appear in the observed $\bar{\nu}_e$. Super-Kamiokande's energy resolution for positrons in this energy range is 10% or better [24]. The $\bar{\nu}_e$ energy can be determined from the positron energy, and hence the energy resolution of Super-Kamiokande permits the detection of this secondary effect due to the sudden compactification of the progenitor core during the quark hadron phase transition. A third feature of the QCD phase transition is the transient increase in the $\bar{\nu}_e$ energies and luminosity, occurring ~ 0.1 s after the phase transition, as a result of accretion onto the remnant. This feature is most readily observable for the normal mass hierarchy scenario.

Discussion and Summary.— Core-collapse SNe can be used to probe the state of matter at high baryon densities, beyond the reach of heavy-ion programs at RHIC and LHC, and complementary to those that will be studied with FAIR at GSI Darmstadt. Using the MIT bag model, Ref. [14] numerically investigated the quark-hadron phase transition during the early post-bounce phase of core-collapse SNe, demonstrating a striking burst of $\bar{\nu}_e$ associated with the phase transition. We show that this burst is clearly detectable from the next Galactic core-collapse at the current neutrino detectors IceCube and Super-Kamiokande.

We have discussed three observational features of the QCD neutrino burst. The QCD phase transition results in a clear and sharp rise in the signal rates at neutrino detectors, providing accurate measurements of the energetics and timing of the QCD neutrino burst. Super-Kamiokande also measures the energies of the neutrinos, revealing the increase in average neutrino energies predicted to occur during the QCD burst. Finally, the increased accretion after the phase transition is visible in neutrinos. Importantly, the energetics and delay of the QCD neutrino burst with respect to the deleptonization burst contain correlated information about the hadronic and quark EoSs, the progenitor model, and the critical conditions for the quark-hadron phase transition. If the neutrinos from the next Galactic SN reveal any of these features, it would not only be strong evidence for the presence of quark matter in neutron stars but could additionally pin down the first order phase transition line on the QCD phase diagram.

Finally, the CCSN rate in our Galaxy is estimated by

various methods, some of which are more direct than others, to be 2–4 per century (see, e.g., [25] and reference therein). With the ultimate the supernovae occurrence determined by Poisson statistics, the chance to detect a SN within a few decades is encouraging.

In conclusion, our study confirms once more the crucial role of astrophysical messengers played by neutrinos during a stellar collapse. It is fascinating to realize that in such extreme conditions, weakly-interacting particles, like neutrinos, could become a powerful tool to learn about quarks and the nature of the strong interactions among them.

We thank John Beacom and Georg Raffelt for useful discussions. B.D. acknowledges support from the Deutsche Forschungsgemeinschaft under grant TR-27 Neutrinos and Beyond and the Cluster of Excellence Origin and Structure of the Universe. T.F. and M.L. are supported by the Swiss National Science Foundation grant. no. PP002-124879/1 and 200020-122287 and by CompStar, a research networking program of the European Science Foundation. S.H. thanks the hospitality of the Werner-Heisenberg-Institut, where part of this work took place. I. S. is supported by the Helmholtz Research School on Quark Matter. J. S. is supported by the Heidelberg Graduate School of Fundamental Physics.

-
- [1] M. Malek *et al.* [Super-Kamiokande Collaboration], *Phys. Rev. Lett.* **90**, 061101 (2003)
 - [2] S. Ando and K. Sato, *New J. Phys.* **6**, 170 (2004)
 - [3] S. Horiuchi, J. F. Beacom and E. Dwek, *Phys. Rev. D* **79**, 083013 (2009)
 - [4] S. E. Woosley, A. Heger and T. A. Weaver, *Rev. Mod. Phys.* **74**, 1015 (2002).
 - [5] T. Totani, K. Sato, H. E. Dalhed and J. R. Wilson, *Astrophys. J.* **496**, 216 (1998).
 - [6] A. S. Dighe, M. T. Keil and G. G. Raffelt, *JCAP* **0306**, 005 (2003).
 - [7] F. Halzen and G. G. Raffelt, arXiv:0908.2317 [astro-ph.HE].
 - [8] A. Dighe, *J. Phys. Conf. Ser.* **136**, 022041 (2008)
 - [9] M. Takahara and K. Sato, *Prog. Theor. Phys.* **80**, 861 (1988).
 - [10] J. A. Pons, A. W. Steiner, M. Prakash and J. M. Lattimer, *Phys. Rev. Lett.* **86**, 5223 (2001).
 - [11] K. S. Hirata *et al.*, *Phys. Rev. D* **38**, 448 (1988).
 - [12] N. A. Gentile *et al.*, *Astrophys. J.* **414**, 701 (1993).
 - [13] K. Nakazato, K. Sumiyoshi and S. Yamada, *Phys. Rev. D* **77**, 103006 (2008).
 - [14] I. Sagert *et al.*, *Phys. Rev. Lett.* **102**, 081101 (2009).
 - [15] M. Kachelriess *et al.*, *Phys. Rev. D* **71**, 063003 (2005).
 - [16] H. Duan, G. M. Fuller, J. Carlson and Y. Z. Qian, *Phys. Rev. Lett.* **100**, 021101 (2008).
 - [17] G. Sigl *et al.*, *Nucl. Phys. Proc. Suppl.* **188**, 101 (2009).
 - [18] S. Hannestad, G. G. Raffelt, G. Sigl and Y. Y. Y. Wong, *Phys. Rev. D* **74**, 105010 (2006)
 - [19] A. S. Dighe and A. Y. Smirnov, *Phys. Rev. D* **62**, 033007 (2000).

- [20] G. L. Fogli *et al.*, Phys. Rev. D **78**, 033010 (2008).
- [21] B. Dasgupta and A. Dighe, Phys. Rev. D **77**, 113002 (2008)
- [22] A. Mirizzi, G. G. Raffelt and P. D. Serpico, JCAP **0605**, 012 (2006)
- [23] A. Marek, H. T. Janka and E. Mueller, arXiv:0808.4136 [astro-ph].
- [24] M. Nakahata *et al.* [Super-Kamiokande Collaboration], Nucl. Instrum. Meth. A **421**, 113 (1999)
- [25] R. Diehl *et al.*, Nature **439**, 45 (2006)